APPLIED ORGANOMETALLIC CHEMISTRY
Appl. Organometal. Chem. **14**, 197–211 (2000)

Spectroscopic Characterization and Biological Activity of L-Methionyl-L Histidinato Complexes of $R_2Sn(IV)$ Ions (R = Me, nBu, Ph) and X-ray Structure of $Me_2SnMetHis \cdot 0.5MeOH$

M. A. Girasolo,* T. Pizzino, C. Mansueto, G. Valle and G. C. Stocco
[1]Dipartimento di Chimica Inorganica and Facoltà di Farmacia, Università di Palermo, Viale delle Scienze, Parco d'Orleans, 90128 Palermo, Italy
[2]Istituto di Zoologia, via Archirafi 20, 90123 Palermo, Italy
[3]Centro di Studi sui Biopolimeri, Dipartimento di Chimica Organica, Università di Padova, via Marzolo 1, 35131 Padova, Italy

Complexes of L-methionyl-L-histidine (H_2MetHis) with $R_2Sn(IV)$ ions (R = Me, nBu, Ph) have been synthesized. The crystal and molecular structures of $Me_2SnMetHis \cdot 0.5MeOH$ have been determined by X-ray diffraction. The title compound contains two crystallographically independent molecular units possessing the same trigonal-bipyramidal geometry at tin, each dimethyltin(IV) moiety being coordinated by the terminal amino nitrogen, deprotonated peptide nitrogen and terminal carboxylate group, neither the imidazole nor thioether groups being involved in bonding.

IR spectroscopy was used to probe the structure of the complexes in the solid state, and the structure in solution (CD_3OD) was assessed by ^1H and ^{13}C NMR. $Me_2Sn(IV)$dipeptide complexes appear to be undissociated and to retain a pentacoordinated structure. Rotamer population of C-terminal histidine was determined by analysis of vicinal coupling constants and side-chain orientations have been interpreted with a view to potential applications of the compounds as recognition agents.

Biological activity was tested on Ascidian embryos of *Ciona intestinalis* at different stages of development. Copyright © 2000 John Wiley & Sons, Ltd.

Keywords: diorganotin(IV); methionylhistidine; X-ray structure; IR; ^1H and ^{13}C NMR spectra; rotamer population; development; Ascidiaceae

Received 11 June 1999; accepted 18 October 1999

INTRODUCTION

The imposition by metal ions of conformational constraints on peptidic ligands, leading to complex molecules whose structure acts as a template orienting side chains in such a way that they act as recognition elements towards a receptor substrate, has been proposed as a key strategy in the development of structure-based design of peptidomimetics.[1]

Moreover, the task of designing artificial nucleases by combining in one molecule a DNA-binding moiety, (represented by a rhodium intercalator), and a reactive domain (represented by a tethered metallopeptide modeled on natural hydrolytic enzymes), has been successfully accomplished by Barton and co-workers.[2]

The title compounds refer to diorganotin(IV), a moiety known to possess antitumor activity,[3] and the dipeptide L-methionyl-L-histidine (Fig. 1), which along with other methionine–containing peptides is able to coordinate transition–metal ions. In the case of biologically relevant platinum(II), binding competition between histidine and methionine side chains has been investigated.[4] As for related applications, it has been demonstrated in immobilized metal ion affinity chromatography (IMAC) that peptides containing both methionine and histidine, possessing a high affinity for metal

* Correspondence to: M. A. Girasolo, Dipartimento di Chimica Inorganica, Università di Palermo, Viale delle Scienze, Parco d'Orleans, 90128 Palermo, Italy.
Contract/grant sponsor: Ministero per l'Università e la Ricerca Scientifica (Roma).

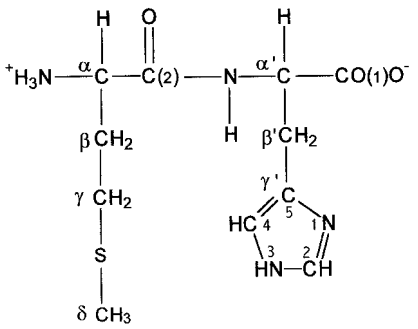

Figure 1 A representation of H_2MetHis, with numbering of atoms.

ions immobilized on stationary phases, can be effectively separated and purified; hence a potential purification strategy is to attach a metal-chelating peptide, either chemically or biosynthetically, to the N-terminus of a protein. In this context, H_2MetHis might behave as a purification device for recombinant proteins since the specific nucleotide sequence can be ligated to the exon coding for the desired protein.[5]

Iron-thiolate-induced oxidation of methionine to methionine sulfoxide by intramolecular catalysis by histidine is an example of mutual interaction mediated by metal ions.[6]

The crystal structure of Me_2SnMetHis·0.5MeOH exemplifies the important role played by hydrogen-bonding interactions in determining the molecular packing in the solid.[7] Indeed, the complex reported in this work, along with those of tryptophan-containing peptides previously reported,[8] appears to adopt a self-assembly pattern, mediated by solvent molecules, which might be indicative of the potential role of these peptide complexes as supramolecular synthons. Moreover, it is noteworthy that since neither the imidazole ring of histidine nor the thioether group of methionine is bound to the metal ion, they must act as pendant arms extending on the exterior part of the molecule; hence the possibility exists that histidine side chains, in particular, may effectively recognize biomolecules such as DNA, as in 'zinc finger' proteins,[9] and therefore display biological activity.

EXPERIMENTAL

L-methionyl-L-histidine (H_2MetHis) was obtained from Bachem (Switzerland) and used without further purification. Me_2SnO and Ph_2SnO were obtained by hydrolysis of Me_2SnCl_2 and Ph_2SnCl_2. The solvent (MeOH) was dried by standard methods.

The compounds were synthesized by addition of freshly prepared R_2SnO (2 mmol) (R = Me, nBu, Ph) to a solution of the stoichiometric amount of L-methionyl-L-histidine (2 mmol) in 50 ml of anhydrous methanol, followed by refluxing for 4 h. The solvent was reduced to a small volume in a rotary evaporator and colorless crystals of Me_2Sn-MetHis suitable for X-ray analysis were obtained immediately, while nBu_2SnMetHis and Ph_2SnMetHis were obtained as white solids by addition of diethyl ether. The solids were filtered off, washed with MeOH and dried *in vacuo* over P_4O_{10}.

Elemental microanalyses for C, H, N and S were performed by the Department of Inorganic, Organometallic and Analytical Chemistry, University of Padova, Italy.

Me_2SnMetHis·0.5MeOH: Found: C, 35.96; H, 5.29; N, 12.92; S, 6.96. Calcd: C, 36.10; H, 5.38; N, 12.47; S, 7.14%.

nBu_2SnMetHis·H_2O: Found: C, 42.64; H, 6.76; N, 10.22. Calcd. C, 42.63; H, 6.78; N, 10.47%.

Ph_2SnMetHis·1.5H_2O: Found: C, 47.15; H, 4.83; N, 9.38; S 5.45. Calcd: C, 47.28; H, 5.00; N, 9.59; S, 5.49%.

Infrared spectra were recorded for Nujol mulls (4000–180 cm^{-1}) with a Perkin-Elmer model 983G instrument.

^{1}H and proton-decoupled ^{13}C NMR spectra were recorded at room temperature, on a Bruker AC250E spectrometer operating at 250.1 MHz for ^{1}H and at 62.89 MHz for ^{13}C. Tetramethylsilane (TMS) was used as internal standard.

Standard programs were used to acquire phase-sensitive 2D COSY spectra which were recorded at room temperature (25±1 °C); sweep width was typically 2380.95 Hz, 256 free induction decays were recorded in 512 data points, each of which consisted of 64 scans.

Spectra were simulated using the RACCOON program (University of Wisconsin).

Concentrations were 10^{-2} M for Me_2SnMetHis and nBu_2SnMetHis; nearly saturated solutions were used for the less soluble Ph_2SnMetHis.

The solvent content in the complexes was authenticated by thermogravimetric analysis using a Mettler TA 3000 system in a pure nitrogen atmosphere in the temperature range 35–450 °C.

Biological material and methods

Adult specimens of *Ciona intestinalis* (Urochordata), collected from the Gulf of Palermo and its vicinity, were identified according to Berrill.[10] Male and female gametes were removed from the gonoducts of dissected animals and transferred into Syracuse dishes. The eggs were reared in Millipore-filtered seawater. Dry sperm was diluted before insemination. Fertilized eggs at the two-cell stage were incubated in 10^{-5} or 10^{-7} M solutions of H_2MetHis and of the complexes Me_2SnMetHis, nBu_2SnMetHis and Ph_2SnMetHis (positive controls) and in seawater (negative controls). All the experiments were performed at 22 °C. The pH of the solutions was controlled and maintained at the normal pH of seawater (7.75–7.80).

In vivo observations were made with a Leitz microscope and photographs were taken with a Leitz Ortoplan microscope, using an Ilford FP4 Plus film.

X-ray crystallography

Unit cell dimensions were determined by X-ray diffraction and refined using the angular settings of 24 automatically centered reflections in the range $12° < 2\theta < 24°$. Intensity data were recorded using a θ–2θ scan from 4.5 to 56.0 °.

Intensities were measured with a Philips PW1100 diffractometer (T = 293 K); no absorption correction was applied and the structure was solved by direct methods using *SHELX 86*[11] and refined by full-matrix least-squares techniques with *SHELX 76*[11] using 2649 reflections having $F > 3\sigma(F)$ and 414 refined parameters. The molecular graphics program used was *ORTEP*$_{12}$. Hydrogen atoms were calculated but not refined. Data collection details and results of the refinements are summarized in Table 1. Fractional coordinates for the complexes are given in Table 2.

Complete atomic coordinates, thermal parameters and bond lengths and angles have been deposited at the Cambridge Crystallographic Data Centre, 12 Union Road, Cambridge CB2 1EZ, UK, as supplementary publication no. CCDC.

Table 1 Crystal data for $[Me_2SnMetHis]_2{\cdot}CH_3OH$

Formula	$C_{27}H_{48}N_8O_7S_2Sn_2$
Mol.wt	898.28
Crystal system	Orthorombic
Space group	$P2_12_12_1$
Crystal dimensions (mm^3)	$0.3 \times 0.3 \times 0.3$
a (Å)	20.058(2)
b (Å)	20.217(2)
c (Å)	9.207(2)
α (deg)	90
β (deg)	90
γ (deg)	90
V (Å^3)	3733(1)
Z	4
D_c ($Mg\,m^{-3}$)	16.0
λ (Mo (Å)	0.71073
μ (cm^{-1})	14.99
No. of measured reflections	5083
No. of independent reflections	5020
No. of observed reflections	2649
F (000)	1816
R	0.069
wR	0.071
w	$1.0/[\sigma^2(F) + 0.0072F^2]$
G	0.844
Goodness of fit = $\sum[w(F_0-F_c)^2)]^{1/2}/(N\text{-}P)$	

RESULTS AND DISCUSSION

Characterization of the complexes in the solid state

Thermogravimetric analysis

The thermal decomposition of the complexes was investigated by thermogravimetry (TG) and differential TG (DTG) techniques to authenticate the nature and extent of solvent molecules in the solid.

The Me_2SnMetHis·0.5MeOH for which the X-ray crystal structure has been solved undergoes a mass loss corresponding to 3.74% in the 35–100 °C range (DTG 55 °C) in agreement with the 3.57% value expected for 0.5 mol CH_3OH per formula unit.

For the identification and quantification of solvent molecules in the nBu_2SnMetHis·H_2O and Ph_2SnMetHis·1.5H_2O, a comparison was made with the free ligand (Bachem, lot no. 508463). For the free ligand, a first mass loss was recorded in the 107–144 °C range (DTG 137 °C) corresponding to 1.53%, followed by a second in the range 144–185 °C (DTG 159 °C) corresponding to a mass loss of 5.75%. Bachem provides the following values for the ligand/water content: 1.5% corresponds to 0.25 mol H_2O per formula unit; 6.0% of formic acid corresponds to 0.4 mol HCOOH per formula unit.

Hence our TGA experimental values are in good agreement with those provided by the manufacturer.

Table 2 Fractional atomic coordinates and equivalent isotropic displacement parameters (Å^2) with ESD (in parentheses)

	x	*y*	*z*	$U_{is/eq}$
Molecule **A**				
Sn(1)	0.06397(6)	0.09017(5)	0.413(1)	0.0562(4)
S(1)	0.0264(3)	−0.2037(3)	0.3228(6)	0.086(2)
O(1)	0.0792(5)	0.1661(5)	0.572(1)	0.059(4)
O(2)	0.101(8)	0.1846(6)	0.803(1)	0.079(5)
O(3)	0.1086(6)	−0.0607(5)	0.71(1)	0.056(4)
N(1)	0.044(1)	−0.0201(8)	0.369(2)	0.120(6)
N(2)	0.1011(6)	0.0377(5)	0.595(1)	0.043(4)
N(3)	0.247(6)	0.1534(6)	0.568(2)	0.057(5)
N(4)	0.311(7)	0.0875(7)	0.438(2)	0.068(5)
C(1)	−0.038(1)	0.116(1)	0.401(3)	0.097(9)
C(2)	0.136(1)	0.119(1)	0.264(2)	0.091(9)
C(3)	0.0974(8)	0.1472(8)	0.703(2)	0.057(6)
C(4)	0.1219(7)	0.0749(7)	0.719(2)	0.047(5)
C(5)	0.0966(7)	−0.0281(7)	0.602(2)	0.047(5)
C(6)	0.0728(8)	−0.0644(7)	0.47(2)	0.045(5)
C(7)	0.1221(8)	−0.113(1)	0.416(2)	0.069(7)
C(8)	0.102(1)	−0.156(1)	0.293(2)	0.083(8)
C(9)	0.054(2)	−0.263(1)	0.459(3)	0.13(1)
C(10)	0.1975(7)	0.0735(7)	0.744(2)	0.051(5)
C(11)	0.2402(7)	0.0911(7)	0.624(2)	0.049(5)
C(12)	0.278(1)	0.0472(8)	0.54(2)	0.066(7)
C(13)	0.29(9)	0.1486(9)	0.471(2)	0.077(8)
Molecule **B**				
Sn(2)	0.45018(5)	0.64608(6)	0.0664(1)	0.0504(3)
S(2)	0.23(4)	0.7297(4)	0.577(1)	0.135(4)
O(4)	0.5009(6)	0.5675(6)	−0.052(1)	0.074(5)
O(5)	0.5184(7)	0.46(6)	−0.058(2)	0.093(6)
O(6)	0.4163(5)	0.5263(5)	0.428(1)	0.057(4)
N(5)	0.3875(6)	0.6833(6)	0.251(1)	0.050(5)
N(6)	0.4343(6)	0.564(6)	0.197(1)	0.046(4)
N(7)	0.2859(7)	0.5011(7)	0.086(2)	0.058(5)
N(8)	0.2779(8)	0.4999(7)	−0.151(1)	0.056(5)
C(14)	0.5386(8)	0.699(1)	0.103(2)	0.075(7)
C(15)	0.383(1)	0.663(1)	−0.097(2)	0.078(8)
C(16)	0.4935(9)	0.507(1)	0.003(2)	0.061(7)
C(17)	0.4561(8)	0.4981(9)	0.144(2)	0.053(5)
C(18)	0.416(7)	0.5702(7)	0.337(2)	0.041(4)
C(19)	0.3947(7)	0.6393(7)	0.38(2)	0.046(5)
C(20)	0.331(1)	0.6429(9)	0.471(2)	0.066(7)
C(21)	0.319(1)	0.709(1)	0.528(3)	0.091(9)
C(22)	0.223(1)	0.676(1)	0.705(5)	0.14(2)
C(23)	0.4003(8)	0.4523(7)	0.129(2)	0.050(5)
C(24)	0.3446(8)	0.4731(8)	0.031(2)	0.049(5)
C(25)	0.3391(9)	0.474(1)	−0.118(2)	0.065(7)
C(26)	0.2506(9)	0.515(1)	−0.027(2)	0.066(7)
O(1)M	−0.2596(7)	0.2147(7)	0.348(2)	0.115(8)
C(1)M	−0.2(1)	0.185(1)	0.36(3)	0.10(1)

Thermogravimetric analysis of nBu_2Sn-MetHis·H_2O and $Ph_2SnMetHis·1.5H_2O$ complexes gave the following indications: solvent molecules were gradually lost up to 200 °C, the dibutyltin(IV) derivative underwent a mass loss of 2.85%, and for the diphenyltin(IV) complex the mass loss was

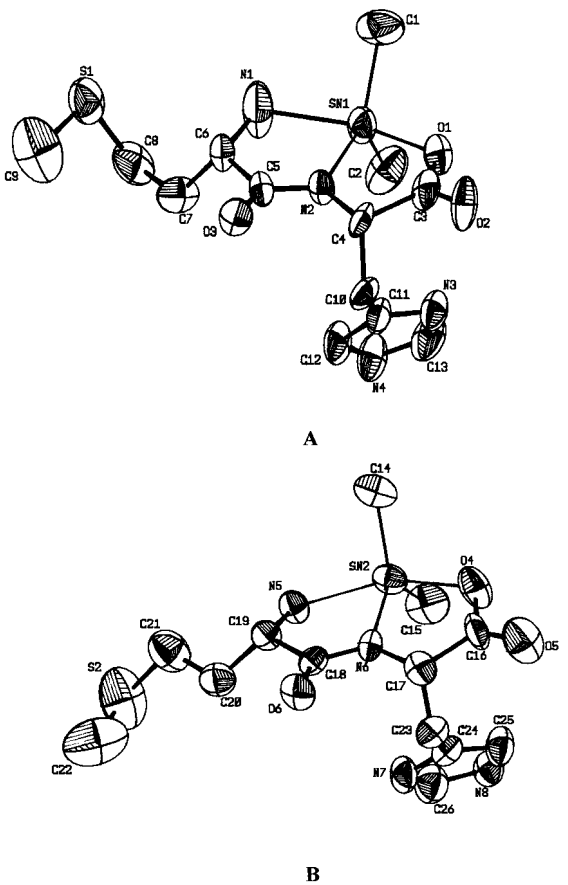

Figure 2 Structure of **A** and **B** molecular units, and atomic numbering scheme.

4.54%. These experimental data indicate that water is present in the complexes, the content in the former complex being slightly less than the value calculated (3.36%) for 1 mol H_2O per formula unit, while in the latter it agrees closely with the calculated value (4.62%) for 1.5 mol H_2O per formula unit.

X-ray crystal structure of $Me_2SnMetHis \cdot 0.5MeOH$

The title compound contains two crystallographically independent molecular units, **A** and **B** (Fig. 2), which have the same basic trigonal-bipyramidal geometry at tin, namely each dimethyltin(IV) moiety is bonded by the terminal amino nitrogen, deprotonated peptide nitrogen and terminal carboxylate group, the chelate dipeptide ligand forming two five-membered chelate rings with the metal ion. Figure 2 shows the molecular structures and the numbering scheme. Selected bond distances and angles are reported in Table 3; they include $Sn–N_{amino}$ = 2.30(2) Å, $Sn–N_{peptide}$ = 2.12(1) Å, $Sn–O_{carboxylate}$ = 2.15(1) Å for molecule **A**, and $Sn–N_{amino}$ = 2.25(1) Å, $Sn–N_{peptide}$ = 2.07(1) Å, $Sn–O_{carboxylate}$ = 2.18(1) Å for molecule **B**; the C-Sn-C angles for the organometallic moiety which, with $N_{peptide}$ defines the equatorial plane, are 124.6(9)° for molecule **A** and 125.7(8)° for molecule **B**. The axial $O_{carboxylate}-Sn-N_{amino}$ angles deviate appreciably from linearity: they are 146.9(6)° and 152.3(5)° for molecules **A** and **B** respectively. In this context, the carboxylate group is acting as a monodentate ligand in an *anti* configuration.

The mean plane of the chelating dipeptide is defined by N(1),C(6),C(5),C(4),O(1) atoms for molecule **A**, showing deviations from planarity of −0.128 Å for N(2) and +0.204 Å for C(3), and by N(5),C(18),N(6),C(16),O(4) atoms for molecule **B**, with deviations from planarity of +0.226 for C(19) and −0.202 for C(17). In C-terminal histidine, the imidazole ring projects obliquely towards the chelate ring and forms an angle of 112.7(5)° in molecule **A** and a larger one [126.4(6)°] in molecule **B**, with the best mean coordination plane. In both instances histidine is present as the NH-3 tautomer, but the imidazole ring is present as two conformers, generated by rotation around the $C^{\alpha'}–C^{\beta'}$ (or $C^{\beta'}–C^{\gamma'}$) bond. The geometry, bond distances and angles of the imidazole ring not involved in bonding to the organometallic moiety, are in agreement with the values found for the free aminoacid.[13a] The conformation of the histidine and methionine residues can be described using the torsion angles in Table 3, (torsion angle nomenclature is according to the IUPAC–IUB Commission on Biochemical Nomenclature[14]). Noticeably for histidine residue χ^1 = N(2)−C(4)−C(10)−C(11) = 52(2)°(**A**) and χ = N(6)−C(17)−C(23)−C(24) = 57(2)°(**B**); $\chi^{2,1}$ = C(4)−C(10)−C(11)−N(3) = 70(2)°(**A**) and $\chi^{2,1}$ = C(17)−C(23)−C(24)−N(7) = −98(2)°(**B**). In the histidine residue with respect to the $C^{\alpha'}–C^{\beta'}$ bond, $C^{\beta'}–C^{\gamma'}$ lies *gauche* relative to $C^{\alpha'}$–CO and $C^{\alpha'}$–N, thus corresponding to the $\mathbf{g}^+$ side-chain conformation. For the methionine residue, two different side-chain conformations are present.

It is noteworthy that sulfur atoms are not involved in bonding to the organometallic moiety; the methionine residue is therefore present in the extended form which closely resembles that found for N-terminal methionine in $Me_2SnMetMet$,[15] whereas the conformational freedom of the histi-

Table 3 Bond distances, bond angles and torsion angles, with ESD in parentheses

Bond distances (Å)			
Molecule **A**			
Sn(1)–O(1)	2.15(1)	Sn(1)-N(1)	2.30(2)
Sn(1)–N(2)	2.12(1)	Sn(1)-C(1)	2.11(2)
Sn(1)–C(2)	2.07(2)	S(1)-C(8)	1.82(2)
S(1)–C(9)	1.82(3)	O(1)-C(3)	1.31(2)
O(2)–C(3)	1.19(2)	O(3)-C(5)	1.22(2)
N(1)–C(6)	1.42(2)	N(2)-C(4)	1.43(2)
N(2)–C(5)	1.33(2)	N(3)-C(11)	1.37(2)
N(3)–C(13)	1.25(3)	N(4)-C(12)	1.41(2)
N(4)–C(13)	1.34(2)	C(3)-C(4)	1.55(2)
C(4)–C(10)	1.54(2)	C(5)-C(6)	1.49(2)
C(6)–C(7)	1.48(2)	C(7)-C(8)	1.48(3)
C(10)–C(11)	1.45(2)	C(11)-C(12)	1.40(2)
Molecule **B**			
Sn(2)–O(4)	2.18(1)	Sn(2)-N(5)	2.25(1)
Sn(2)–N(6)	2.07(1)	Sn(2)-C(14)	2.10(2)
Sn(2)–C(15)	2.05(2)	S(2)-C(21)	1.90(2)
S(2)–C(22)	1.60(4)	O(4)-C(16)	1.34(2)
O(5)–C(16)	1.21(2)	O(6)-C(18)	1.22(2)
N(5)–C(19)	1.49(2)	N(6)-C(17)	1.48(2)
N(6)–C(18)	1.35(2)	N(7)-C(24)	1.40(2)
N(7)–C(26)	1.29(2)	N(8)-C(25)	1.37(2)
N(8)–C(26)	1.31(2)	C(16)-C(17)	1.51(2)
C(17)–C(23)	1.46(2)	C(18)-C(19)	1.51(2)
C(19)–C(20)	1.54(2)	C(20)-C(21)	1.45(3)
C(23)–C(24)	1.49(2)	C(24)-C(25)	1.38(2)
O(1)M–C(1)M	1.35(3)		
Bond angles (deg)			
Molecule **A**			
C(1)-Sn(1)-C(2)	124.6(9)	N(2)-Sn(1)-C(2)	114.7(7)
N(2)-Sn(1)-C(1)	120.5(7)	N(1)-Sn(1)-C(2)	106.0(8)
N(1)-Sn(1)-C(1)	93.6(8)	N(1)-Sn(1)-N(2)	73.4(6)
O(1)-Sn(1)-C(2)	98.9(7)	O(1)-Sn(1)-C(1)	89.8(7)
O(1)-Sn(1)-N(2)	76.6(4)	O(1)-Sn(1)-N(1)	146.9(6)
C(8)-S(1)-C(9)	101(1)	Sn(1)-O(1)-C(3)	117.3(9)
Sn(1)-N(1)-H(2)N(1)	77.0(8)	Sn(1)-N(1)-H(1)N(1)	94(1)
Sn(1)-N(1)-C(6)	115(1)	Sn(1)-N(2)-C(5)	121(1)
Sn(1)-N(2)-C(4)	118.0(9)	C(4)-N(2)-C(5)	120(1)
C(11)-N(3)-C(13)	105(1)	C(12)-N(4)-C(13)	104(1)
O(1)-C(3)-O(2)	123(1)	O(2)-C(3)-C(4)	121(1)
O(1)-C(3)-C(4)	117(1)	N(2)-C(4)-C(3)	109(1)
C(3)-C(4)-C(10)	110(1)	N(2)-C(4)-C(10)	114(1)
O(3)-C(5)-N(2)	124(1)	N(2)-C(5)-C(6)	118(1)
O(3)-C(5)-C(6)	118(1)	N(1)-C(6)-C(5)	111(1)
C(5)-C(6)-C(7)	113(1)	N(1)-C(6)-C(7)	118(1)
C(6)-C(7)-C(8)	117(1)	S(1)-C(8)-C(7)	115(1)
C(4)-C(10)-C(11)	118(1)	N(3)-C(11)-C(10)	125(1)
C(10)-C(11)-C(12)	126(1)	N(3)-C(11)-C(12)	109(1)
N(4)-C(12)-C(11)	105(1)	N(3)-C(13)-N(4)	117(1)
Molecule **B**			
C(14)-Sn(2)-C(15)	125.7(8)	N(6)-Sn(2)-C(15)	117.5(7)
N(6)-Sn(2)-C(14)	116.6(6)	N(5)-Sn(2)-C(15)	97.6(7)
N(5)-Sn(2)-C(14)	100.3(7)	N(5)-Sn(2)-N(6)	75.1(4)
O(4)-Sn(2)-C(15)	93.6(6)	O(4)-Sn(2)-C(14)	93.5(6)

Table 3 (continued)

O(4)-Sn(2)-N(6)	77.2(5)	O(4)-Sn(2)-N(5)	152.3(5)
C(21)-S(2)-C(22)	97(1)	Sn(2)-O(4)-C(16)	115(1)
Sn(2)-N(5)-H(2)N(5)	113.6(9)	Sn(2)-N(5)-H(1)N(5)	102.4(8)
Sn(2)-N(5)-C(19)	110.4(9)	C(19)-N(5)-H(2)N(5)	110(1)
C(19)-N(5)-H(1)N(5)	114(1)	Sn(2)-N(6)-C(18)	121.5(9)
Sn(2)-N(6)-C(17)	118.9(9)	C(17)-N(6)-C(18)	118(1)
C(24)-N(7)-C(26)	105(1)	C(26)-N(8)-H(1)N(8)	128(1)
C(25)-N(8)-H(1)N(8)	127(1)	C(25)-N(8)-C(26)	106(1)
O(4)-C(16)-O(5)	120(1)	O(5)-C(16)-C(17)	121(1)
O(4)-C(16)-C(17)	119(1)	N(6)-C(17)-C(16)	109(1)
C(16)-C(17)-C(23)	112(1)	N(6)-C(17)-C(23)	112(1)
O(6)-C(18)-N(6)	126(1)	N(6)-C(18)-C(19)	114(1)
O(6)-C(18)-C(19)	120(1)	N(5)-C(19)-C(18)	112(1)
C(18)-C(19)-C(20)	115(1)	N(5)-C(19)-C(20)	109(1)
C(19)-C(20)-C(21)	112(1)	S(2)-C(21)-C(20)	116(1)
C(17)-C(23)-C(24)	117(1)	N(7)-C(24)-C(23)	122(1)
C(23)-C(24)-C(25)	131(1)	N(7)-C(24)-C(25)	107(1)
N(8)-C(25)-C(24)	107(1)	N(7)-C(26)-N(8)	115(1)
O(1)M-C(1)M-H(1)CM	113(2)	C(1)M-O(1)M-H1OM	111(1)
Torsion angles (deg)			
Molecule **A**		Molecule **B**	
N(1)-Sn(1)-N(2)-C(4)	−171(1)	N(5)-Sn(2)-N(6)-C(17)	172(1)
O(1)-C(3)-C(4)-C(10)	109(2)	O(4)-C(16)-C(17)-C(23)	124(2)
C(3)-C(4)-C(10)-C(11)	−71(2)	C(16)-C(17)-C(23)-C(24)	57(2)
N(2)-C(4)-C(10)-C(11)	52(2)	N(6)-C(17)-C(23)-C(24)	57(2)
C(4)-C(10)-C(11)-N(3)	70(2)	C(17)-C(23)-C(24)-N(7)	−98(2)
C(4)-C(10)-C(11)-C(12)	−105(2)	C(17)-C(23)-C(24)-C(25)	78(2)
C(10)-C(11)-C(12)-N(4)	−180(1)	C(23)-C(24)-C(25)-N(8)	−178(2)
Sn(1)-N(1)-C(6)-C(7)	−119(1)	Sn(2)-N(5)-C(19)-C(20)	−152(1)
C(9)-S(1)-C(8)-C(7)	−69(2)	C(22)-S(2)-C(21)-C(20)	64(2)
N(1)-C(6)-C(7)-C(8)	−53(2)	N(5)-C(19)-C(20)-C(21)	−63(2)
C(5)-C(6)-C(7)-C(8)	176(1)	C(18)-C(19)-C(29)-C(21)	171(1)
C(6)-C(7)-C(8)-S(1)	−56(2)	C(19)-C(20)-C(21)-S(2)	157(1)

dine residue is restricted by the presence of the metal-complexed core.

Hydrogen bonds play a significant role in determining the crystal packing of the complex (Fig. 3). Monomeric units **A** are interconnected by relatively weak N—H···O hydrogen bonds between the imidazole NH-3 hydrogen donor of one molecule and the peptide CO acceptor oxygen atoms of the next, the former acting as an acceptor of hydrogen bonds from methanol through N(1). Hydrogen-bonding details are reported in Table 4. Molecules **B** are interconnected by direct interaction between the imidazole NH-3 donor and the N(1) acceptor, which brings the two imidazole rings close together in a edge-to-edge fashion. The alternative conformation shown by molecule **B** is presumably dictated by hydrogen-bond formation in the crystal structure.

Molecules **A** and **B** are interconnected by hydrogen bonds promoted by the coordinated amino group of **B**, which is H-bonded to the carboxylate group of **A**, and to a solvent molecule

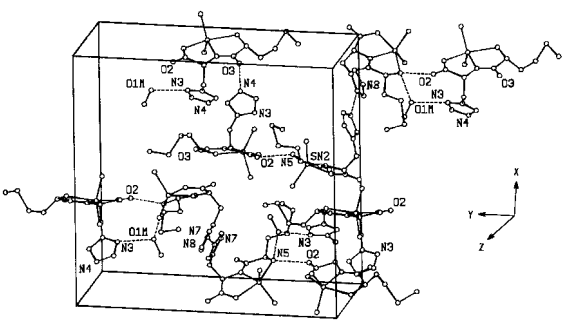

Figure 3 The unit cell of $Me_2SnMetHis{\cdot}0.5MeOH$. Broken lines indicate hydrogen bonds.

Table 4 Hydrogen-bonding distances (Å) and angles (°)

D—H···A	D—H	H···A	D···A	D—H···A
O(1)M—H(1)OM···N(3)[a]	0.95(1)	1.83(1)	2.78(2)	179.3(1)
	0.94[f]	1.84		179.3
N(4)—H(1)N(4)···O(3)[b]	1.11(1)	1.61(1)	2.70(2)	165.8(9)
	1.03	1.69		166.5
N(5)—H(1)N(5)···O(1)M[c]	1.11(1)	1.74(1)	2.80(2)	158.8(8)
	1.03	1.81		159.7
N(5)—H(2)N(5)···O(2)[d]	1.08(1)	1.66(1)	2.72(2)	165.6(8)
	1.03	1.71		166.0
N(8)—H(1)N(8)···N(7)[e]	1.08(1)	1.68(1)	2.74(2)	166.5(9)
	1.03	1.72		166.9

Symmetry codes: [a] $+x-\frac{1}{2}, -y-\frac{1}{2}-1, -z-2$;
[b] $+x-\frac{1}{2}, -y-\frac{1}{2}-1, -z-1$;
[c] $-x-\frac{1}{2}-1, -y-2, +z-\frac{1}{2}$;
[d] $-x-2, +y+\frac{1}{2}, -z-\frac{1}{2}-1$;
[e] $-x-\frac{1}{2}-1, -y-1, +z-\frac{1}{2}$.
[f] The second row of data for each bond gives values normalized according to Refs 16 and 17.

which acts as a bridge between the two entities. Solvent molecules, incorporated in the lattice with a site occupancy of 0.5, exert an effect which is also found in the crystal structures of Me_2SnAla-His·MeOH[15] and Me_2SnTrpAla·MeOH.[8]

In the overall view, the two molecules are arranged as H-bonded chains of monomers, resulting in a 'polymer' whose construction is aided by intermolecular interactions which propagate through the crystal as flattened helices running in an antiparallel fashion with a repeat sequence **AABB** along the (100) axis.

This suggests that conformational constraints exerted by metal ions on peptidic ligands lead to a complex molecule whose core structure acts as a template which orients side-chains in a way that enables them to become recognition elements towards a receptor substrate. 'Zinc finger' proteins are an example, where recognition of DNA is effected by donating an H-bond from histidine NH-3 to N7 of guanine.[9] It is tempting to suggest that small (organo)metaldipeptide complexes such as these reported here may be considered as minimalist supramolecular synthons leading to ordered entities driven by H bonds between imidazole nitrogen atoms of two neighboring components, and that they hold promise of becoming part of a key strategy in the development of structure-based design of peptidomimetics.[1,18]

The goal of reproducing the bioactivity of proteins using smaller molecular structures and of elucidating the relationship between sequence and conformation has recently been pursued.[19] These efforts have focused on the construction of 'peptide-amphiphiles' (amphiphilic sheets and/or helices) with the aim of creating novel biomaterials with distinct protein-like structures and template-assembled synthetic proteins (TASP).

In this context methionine can be used as a 'switchable' residue since it is lipophilic but methionine sulfoxide, reversibly generated, is hydrophilic,[20] the 'amphiphilic order' of residues being the main determinant of the preferred conformation. A comparison of the crystal structure of Me_2SnMetMet,[15] which is disordered, with those of Me_2SnAlaHis[15] and Me_2SnMetHis (this work) shows hydrophilic histidine to be effective in directing molecules towards a more ordered self-assembled crystal structure by means of side-chain–side-chain H-bonded contacts.

In the nBu_2Sn(IV) and Ph_2Sn(IV) derivatives, water molecules are also expected to give a network of intermolecular hydrogen-bond contacts, in the crystal packing of the complexes as exhibited by histidine hydrochloride monohydrate where, besides H bonds involving the imino and amino groups, water hydrogen atoms interact with the carboxylate group.[13b] The role of water molecules in determining peptide folding and creation of supermolecules (β-turns, α-helices) has been demonstrated[21] and recently reassessed for triamide and diamide model systems.[22,23]

Vibrational spectra

The infrared spectra of the water-containing ligand and complexes (Table 5) show one broad ν(OH)

Table 5 Some relevant IR frequencies (cm^{-1}) for $R_2Sn(IV)^{2+}$ complexes with dipeptides[a]

Compound	ν(NH) ν(OH)[b]	Amide I	$\nu_{as}(COO^-)$	$\nu_{sym}(COO^-)$	$\nu_{as}(SnC_2)$	$\nu_{sym}(SnC_2)$
H_2MetHis	3485[b] 3315s 3135m	1643m	1607vs	1402m		
Me_2SnMetHis·0.5CH_3OH	3250m,sh[c] 3110s,bd	1643s	1611s	1402w	568m	532m
nBu_2SnMetHis·H_2O	3493s,bd[b] 3423s,bd[b] 3200m,bd[c] 3110w[c]	1638s	1613s	1400m	556m	514m
Ph_2SnMetHis·1.5H_2O	3400s,bd[b] 3200s,bd[c] 3110w[c]	1640s,bd	1619s	1390m		

[a] sh, shoulder; w, weak; m, medium; s, strong; vs, very strong; bd, broad; as, asymmetric; sym, symmetric.
[b] ν(OH) of water present in the compound.
[c] ν(NH) imidazole, superimposed on $\nu(NH_2)$.

band at 3485 cm^{-1} (H_2MetHis) which is split into two bands in nBu_2SnMetHis (3493 and 3423 cm^{-1}), while giving rise to a much broader band centered at 3400 cm^{-1} for Ph_2SnMetHis. A medium band is also present at δ(H-O-H) $\approx$1650 cm^{-1} in all hydrated compounds.

Vibrations associated with the NH_3^+ group (2145 cm^{-1} in H_2MetHis) are missing in the complexes, and appear as $\nu(NH_2)$ at 3250 cm^{-1} (bd) in Me_2SnMetHis, and at 3200 cm^{-1} (bd) in nBu_2SnMetHis and Ph_2SnMetHis. The ν(NH) vibration due to the NH group of the imidazole ring of histidine, as in the previously reported histidine-containing dipeptides,[24] can be assigned to the sharp peaks at 3315 and 3135 cm^{-1} in H_2MetHis, which, in spite of the fact the imidazole group is not involved in bonding to the organometallic moiety, appear to become broader and shifted to lower frequencies (3200 and 3110 cm^{-1}) in the complexes. The doubling of the ν(OH) band has been observed previously in tBu_2SnGly-Gly·H_2O[25,26] where the water molecule is fixed in the crystal packing by H bonds involving both hydrogen atoms of H_2O and the NH_2 group and the carboxyl and carbonyl oxygen atoms. Extensive H-bonding is probably also responsible for the small shifts in the $\nu_{as}(COO^-)$ and Amide I bands (Table 5), while the Amide II band at 1510 cm^{-1} in H_2MetHis, which involves the peptide group N–H deformation, disappears in the complexes.

Values of $\Delta\nu[= \nu_{as}(COO^-) - \nu_{sym}(COO^-)]$ in the range 209–229 cm^{-1} for all the complexes suggest that the carboxylate groups coordinate, in a monodentate fashion, the organometallic ions,[27] along with the terminal amino groups and deprotonated peptide nitrogen atoms, the tridentate peptide ligand yielding complexes structurally similar to those separately containing either methionine or histidine for which X-ray structures have been determined[13b] where the coordination polyhedra around the tin atom are slightly distorted trigonal bipyramids.

Characterization of the complexes in solution

^{13}C NMR spectra

^{13}C NMR resonances for the free ligand, due to its limited solubility in CD_3OD, were obtained in solutions of CD_3OD to which 10% (v/v) of D_2O was added, and/or by addition of stoichiometric amounts of NaOD. The resonances for the free ligand and the organotin(IV) complexes are reported in Table 6.

Relative to the free dipeptide, the shifts of resonances due to metal coordination have been monitored. A general pattern emerges in the complexes, namely a shift to lower field for all resonances with the exception of the δCH_3 resonance of N-terminal L-methionine which shows minor shifts in the opposite direction. Not unexpectedly the more significant shifts are those relative to the carboxylate and peptide carbonyl groups which are directly involved in bonding, while it is significant that an effectively unchanged position for the SCH-3 resonance rules out

Table 6 ^{13}C chemical shifts[a] for H_2MetHis ligand and complexes[e]

Compound	CO-1	CO-2	$^{\alpha}CH$	$^{\beta}CH_2$	$^{\alpha'}CH$	$^{\beta'}CH_2$	$^{\gamma}CH_2$	$^{\delta}CH_3$	CH-2	CH-4	C-5	R_2Sn (R=Me, nBu, Ph)
H_2MetHis[b]	176.92	171.32	55.07	31.06	56.80	35.36	28.64	15.51	139.21	115.72	135.48	
H_2MetHis[c]	176.42	170.32	53.63	29.64	55.94	31.80	28.03	15.04	134.88	118.13	132.46	
Me_2SnMetHis[d]	179.28	175.49	54.83	31.42	57.68	32.93	29.65	14.93	135.78	119.98	133.11	−1.28; −1.14
nBu_2SnMetHis[d]	179.59	175.86	55.17	31.46	58.03	32.98	29.89	14.87	135.87	119.97	133.60	$^{\alpha}C$ = 28.36–27.86 $^{\beta}C$ = 28.04–27.59 $^{\gamma}C$ = 19.55–20.55 $^{\delta}C$ = 13.90
Ph_2SnMetHis[d]	179.18	175.23	54.90	31.38	57.97	32.11	30.46	14.74	135.99	117.86	134.56	C_1 = 137.54 $C_{2,6}$ = 136.53–136.35 $C_{3,5}$ = 130.35–130.09 C_4 = 131.82–131.70

[a] In ppm from TMS.
[b] Solvent: CD_3OD + NaOD.
[c] Solvent: CD_3OD + D_2O.
[d] Solvent: CD_3OD.
[e] For numbering of carbon atoms, see Fig. 1.

Table 7 ^{1}H chemical shifts[a] (δ) and coupling constants (J) for H_2MetHis ligand and complexes with $R_2Sn(IV)^{2+}$

Compound	$^{\alpha}CH$	$^{\beta}CH_2$	$^{\alpha'}CH$	$^{\beta'}CH_2$	$^{\gamma}CH_2$	$^{\delta}CH_3$	CH-2	CH-4	R_2Sn (R=Me, Bu, Ph)	$\lvert^2J(^{119}Sn,^1H)\rvert$[b] $\lvert^2J(^{117}Sn,^1H)\rvert$[b]
H_2MetHis[c,d]	3.97(t)	2.07(m)	4.45(dd)	3.23(dd) 3.13(dd)	2.59(t)	2.11(s)	8.19(s)	7.14(s)		
H_2MetHis[d,f]	3.47(dd)	1.98(m) 1.77(m)	4.37(dd)	3.15(dd) 3.01(dd)	2.53(t)	2.10(s)	7.42(s)	6.80(s)		
Me_2SnMetHis[g]	3.50(dd)	2.34(m) 1.77(m)	4.27(t)	3.22(dd) 3.07(dd)	2.55(m)	2.03(s)	7.44[j](s)	6.63[j](s)	+0.16 +0.52	81.32–77.89 78.23–74.95
nBu_2SnMetHis[h]	3.58(dd)	2.47(m) 1.90(m)	4.38(t)	3.29(dd) 3.17(dd)	2.62(m)	2.13(s)	7.56(s)	6.75(s)	$\delta(CH_3)$ = 0.90(t) $\delta(CH_2)_n$ = 1.04–1.58	
Ph_2SnMetHis[i]	3.55(dd)	2.45(m) 1.90(m)	4.52(t)	3.23(t) 3.16(t)	2.58(m)	2.00(s)	6.85(s)	6.68(s)	$H_{2,6}$ = 7.37 $H_{3,5}$ = 7.47 H_4 = 7.20	

Abbreviations: s, singlet; d, doublet; dd, doublet of doublets; t, triplet; m, multiplet.
[a] In ppm from TMS. [b] In Hz. [c] Solvent: CD_3OD + D_2O. [d] Solvent: CD_3OD + NaOD. [e] $|J_{AB}|$ = 15.0 Hz. [f] $|J_{AB}|$ = 14.0 Hz. [g] $|J_{AB}|$ = 14.2 Hz. [h] $|J_{AB}|$ = 14.4 Hz.
[i] $|J_{AB}|$ = 13.8 Hz. [j] $J_{2,4}$ = 1.0 Hz.

thioether coordination in such complexes. For the presence in solution of the tautomeric forms of the imidazole ring of histidine, reference was made to a study[28] of the characteristic pH-dependent shifts of imidazole carbon atoms, supported by theoretical calculations on histidine, which has been used to determine the tautomeric equilibrium. From these studies as well as from a more recent $^{1}H–^{13}C$ CT-HSQC investigation, the evidence emerges that the NH-3 tautomer is favored[29] in neutral solution. In our experiments a slight broadness of the C(4) and C(5) resonances, especially in $Me_2SnMetHis$, was observed. This gives some indication, being the resonances an average of the two forms, that such an equilibrium is operating in our systems.

Structural details for the complexes in CD_3OD solutions, i.e. determination of C-Sn-C bond angles for the organometallic moieties, have been extracted by evaluating $|^{n}J(^{119}Sn,^{13}C)|$ and by use of the relationships of Lockhart and Manders[30] and Holecek *et al.*[31]

The organometallic moieties of the complexes in solution show coupling constants which may be related to the coordination number of the tin atom and to the C-Sn-C angles for the specimen in solution. For $Me_2SnMetHis$, $^{1}J = 627.5$ Hz, so the C-Sn-C angle is calculated to be 132 °.

For $nBu_2SnMetHis$, the chemical shifts for the carbon atoms of the organometallic moiety have been assigned in relation to the diagnostic values of the ^{n}J coupling constants, $|^{1}J(^{119}Sn,^{13}C)| = 560$ Hz and $|^{1}J(^{117}Sn,^{13}C| = 532$ Hz, $|^{2}J(^{119}Sn,^{13}C)| = 23$ Hz and $|^{3}J(^{119}Sn,^{13}C)| = 80$ Hz, ^{2}J being the smallest and ^{1}J the highest among the ^{n}J values.

For the determination of the structure of n-dibutyltin(IV) the values of both $|^{1}J(^{119}Sn,^{13}C)|$ and $|^{1}J(^{117}Sn,^{13}C)|$ are in agreement with the values proposed by Holecek *et al.*[31] for pentacoordinated compounds; the angles C^{α}-Sn-$C^{\alpha} = 130.7$ ° and 127.9 °, respectively, have been calculated.

It is noteworthy that both the ^{13}C and ^{1}H NMR spectra present a pattern which is found in all $R_2Sn(IV)$ dipeptide complexes, namely the splitting of resonances due to the organometallic moiety, while a single set of resonances relative to the ligand is preserved; the chirality of the complexes is responsible for the appearance of two magnetically non-equivalent R_2Sn resonances.

^{1}H NMR spectra

For the free ligand ($CD_3OD–D_2O$, $CD_3OD–NaOD$), the resonances of the individual amino acids were assigned, according to Wüthrich,[32] to the previously reported methionine- and histidine-containing ligands and complexes[13] by analysis of the two-dimensional $^{1}H–^{1}H$ correlation contour plot (COSY spectrum) for $Me_2SnMetHis$, and are in good agreement with data reported by Sheldrick[4b] for the ligand in D_2O at pD = 6.7. They are reported in Table 7 and Fig. 4.

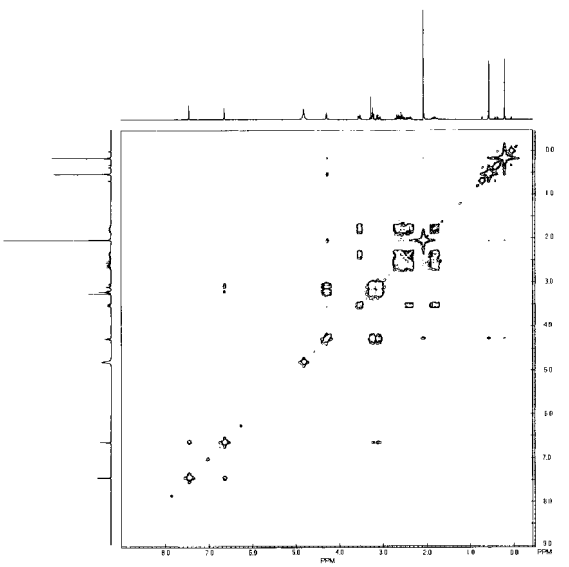

Figure 4 Two-dimensional contour plot of $^{1}H–^{1}H$ correlation spectrum (COSY) of $Me_2SnMetHis·0.5MeOH$.

The addition of equimolar amounts of NaOD to $H_2MetHis$ affords a better resolution of the $^{\beta}CH_2$ signals of methionine. Metallation by the organometallic moiety, relative to the anionic form of the ligand (NaOD added), showed a downfield shift for $^{\alpha}CH$ which is larger in the case of $nBu_2SnMetHis$ and $Ph_2SnMetHis$ derivatives, while $^{\alpha'}CH$ resonances are shifted slightly upfield for $Me_2SnMetHis$, showing, in both one- and two-dimensional (COSY) spectra, a coupling of the $^{\alpha'}CH$ proton of histidine with the ^{119}Sn nucleus of 33 Hz. This finding has also been reported for coordination of the $Me_2Sn(IV)$ ion in aqueous solution with dipeptides such as glycylglycine and glycylhistidine.[33] An additional connectivity is shown in the COSY spectrum between CH-4 and $^{\beta'}CH_2$ protons. For $^{\beta}CH_2$ and $^{\beta'}CH_2$ downfield shifts are generally observed. It is noteworthy that neither the γ nor the δ protons of methionine show any significant shift, which rules out coordination by the thioether group. It is of some interest that the CH-2 and CH-4 resonances (of the imidazole ring) show minor shifts relative to the anionic form of the ligand: whereas for $Me_2SnMetHis$ it is only the

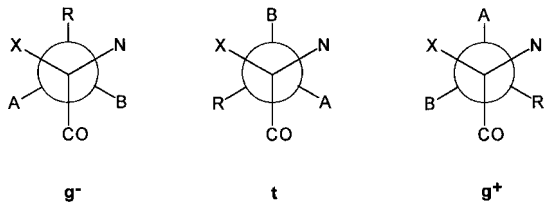

Figure 5 Side-group rotamers where A, B and X are protons: $\mathbf{g}^-$, *gauche* rotamer; **t**, *trans* rotamer; $\mathbf{g}^+$, *gauche*, most-hindered, rotamer.

CH-4 resonance which is shifted to higher field, for $nBu_2SnMetHis$ CH-2 is shifted to lower field by 0.14 ppm and CH-4 to higher field by 0.05 ppm, and in $Ph_2SnMetHis$ both CH-2 and CH-4 resonances are shifted to slightly higher field by 0.57 and 0.12 ppm respectively. A survey of complexes of dipeptides bearing histidine as the C-terminus,[34] where N(1) of the imidazole group bonds to the metal ion, presents the same pattern of upfield shifts of CH-2 and CH-4 protons. Taking into account the large steric hyndrance which is expected for the Ph_2Sn(IV) moiety, it seems unlikely that such bonding takes place in our compound. As previously suggested,[35] side-chain inter- or intramolecular interactions between aromatic rings may induce through-space chemical shift effects.

Considering the conformation of the complexes in solution, as previously observed,[8] whereas in the free ligand the peptide backbone is predominantly present in a flexible extended form, in the complexes chelation by amino, peptide nitrogens and carboxylate groups provides a stiff backbone; therefore it is attached side-chain interactions which play a crucial role in determining which conformation is preferred. The conformation in solution of non-coordinated histidine side chains was estimated by ^{1}H NMR analysis of vicinal proton coupling constants about the $^{\alpha'}CH–^{\beta'}CH_2$ bond. ^{1}H NMR spectra are time-averaged over three predominant staggered rotamers, as illustrated in Fig. 5. The three-spin ABX system generated by $^{\alpha'}CH$ and diastereotopic $^{\beta'}CH_2$ protons was examined; J_{AX} and J_{BX} coupling constants were determined and related to the mole fractions of each rotamer according to the procedure followed by Martin and co-workers[36] (Table 8).

From the conformational studies, the following conclusions can be drawn concerning the conformations adopted by C-terminal histidine relative to the free dipeptide.

In the free dipeptide, whether in the neutral or monoanionic form, rotamer $\mathbf{g}^-$ predominates among the three staggered ethanic rotamers. In the monoanionic form of the dipeptide a slight increase of $\mathbf{g}^-$ and **t** rotamers is observed, relative to the free dipeptide, at the expense of the $\mathbf{g}^+$ rotamer. Following complexation with the organometallic moieties a dramatic increase of the $\mathbf{g}^+$ rotamer is observed, whereby the 5-imidazolyl group appears to be directed towards the coordination plane, consistently with the X-ray structural information obtained for $Me_2SnMetHis$ in the solid state.

For the dimethyltin(IV) moiety, the $|^2J(^{119}Sn,^1H)|$ values are reported in Table 7; C-Sn-C bond angles obtained by Lockhart and Manders' relationship[37] were 132 ° and 129 ° for the two magnetically nonequivalent CH_3(Sn) resonances. The angle appears to be slightly higher than the C-Sn-C angles found for the two crystallographically independent units.

Results of biological testing

The effects of $H_2MetHis$ and its diorganotin

Table 8 Coupling constants and rotamer populations

			Population (mol mol^{-1})		
	J_{AX}[a] (Hz)	J_{BX}[a] (Hz)	$\mathbf{g}^{-a}$	$\mathbf{t}^a$	$\mathbf{g}^{+a}$
$H_2MetHis$[b]	5.2	6.8	0.40	0.26	0.34
$H_2MetHis$[c]	5.5	7.5	0.45	0.30	0.25
$Me_2SnMetHis$	4.0	4.0	0.15	0.15	0.70
$Bu_2SnMetHis$	4.5	4.2	0.16	0.19	0.64
$Ph_2SnMetHis$	3.4	3.6	0.11	0.09	0.79

[a] J_{AX}, J_{BX} and rotamer fractions for C-terminal histidine.
[b] Solvent: $CD_3OD + D_2O$.
[c] Solvent: CD_3OD + NaOD.

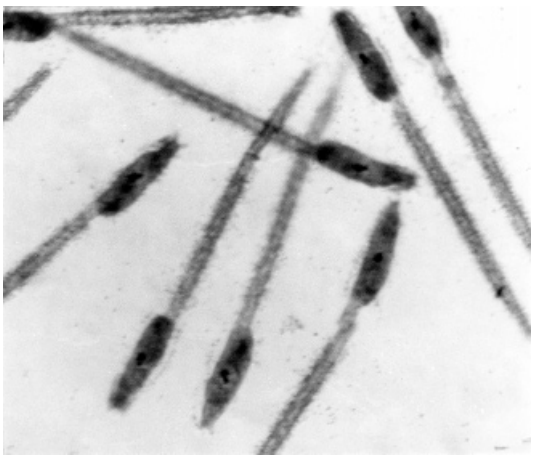

Figure 6 Larvae of *Ciona intestinalis* (controls).

derivatives on *Ciona intestinalis* embryonic development were tested at different concentrations.

Negative controls

As previously observed, for fertilized eggs of *Ciona intestinalis*[38] embryonic development results in the following stages during 24 h: 2, 4, 8, 16, 32, 64 and 128 cells up to gastrula, neurula, tailbud and swimming larva. The last of these possesses a nervous system with two sensitive black spots (Fig. 6).

Treatment with H_2MetHis and diorganotin derivatives

The results are reported in Table 9. Embryo development analysis indicates:

(a) The eggs incubated at the two-cell stage in H_2MetHis free dipeptide develop 50% normal larvae and 50% larvae with twisted tails in 10^{-5} M solution (Fig. 7). The percentage of normal larvae increases in 10^{-7} M solution (80%).

(b) Me_2SnMetHis does not exert any effect on the embryonic development at either 10^{-5} or 10^{-7} M concentration; this result is somewhat unexpected since the activity of the complex species seems to compensate for the adverse effect exerted by the ligand itself.

(c) nBu_2SnMetHis is more toxic than Ph_2SnMetHis, exerting its effect on early events of development, since it promotes inhibition at the mitotic stages, as demonstrated by the fact that 50% of the eggs cease cleavage at anomalous 16–32-cell stages in 10^{-5} M nBu_2SnMetHis solution and 50% develop up to early gastrula (Fig. 8a). Moreover, the nBu_2SnMetHis derivative is toxic at

Table 9 Development of *Ciona intestinalis* eggs in seawater solutions of diorganotin dipeptides treated from two-cell stage up to larva[a]

		Development stage					
Compound	Conc (mol l^{-1})	Anomalous 16-32 blastomeres	Early gastrulae	Anomalous neurulae	Anomalous tailbuds	Anomalous larvae	Swimming larvae
H_2MetHis	10^{-5}	50				50	50
	10^{-7}					20	80
Me_2SnMetHis	10^{-5}						100
	10^{-7}						100
nBu_2SnMetHis	10^{-5}		50				
	10^{-7}			100			
Ph_2SnMetHis	10^{-5}				100		
	10^{-7}						100
Controls							100

[a]Percentage of eggs arrested at an intermediate stage, or developed to swimming larvae (last column), from five experiments.

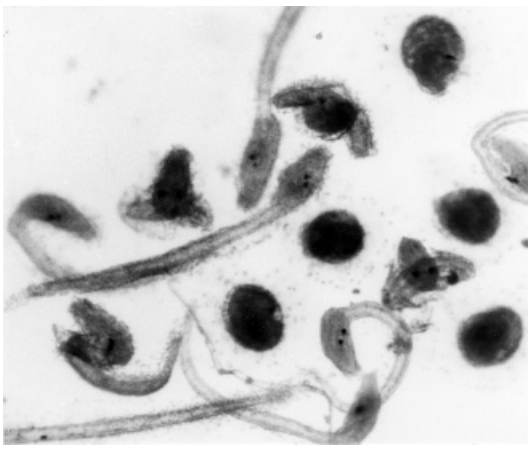

Figure 7 *Ciona intestinalis* anomalous and normal larvae derived from the two-cell stage, incubated in 10^{-5} M H_2MetHis solution.

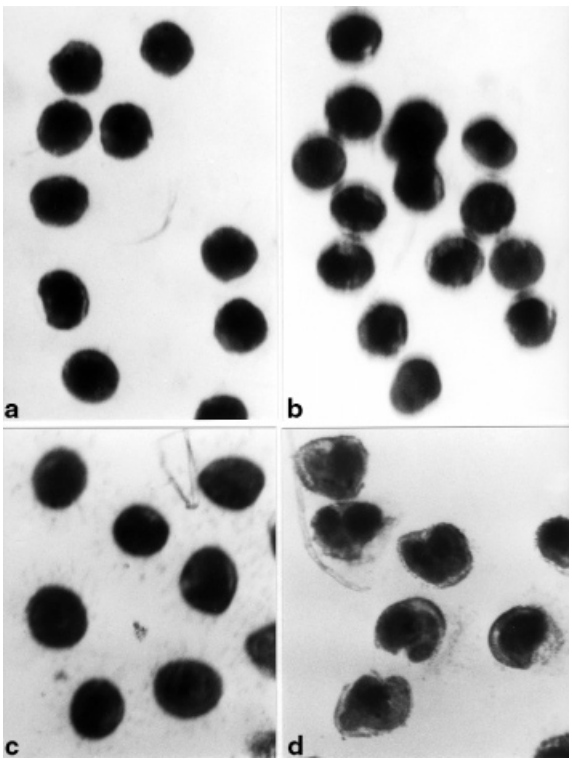

Figure 8 *Ciona intestinalis*. (a) Blocked at the 16–32 cell stage; the fertilized eggs had been incubated in 10^{-5} M nBu_2Sn-MetHis solution at the two-cell stage. (b) Anomalous neurulae derived from the two-cell stage, incubated in 10^{-7} M nBu_2Sn-MetHis solution. (c) Anomalous tailbuds derived from incubation at the two-cell stage in 10^{-5} M $Ph_2SnMetHis$ solution. (d) Anomalous larvae in ovular envelopes derived from the two-cell stage incubated in 10^{-5} M $Ph_2SnMetHis$ solution.

10^{-7} M, (Fig. 8b) as anomalous neurulae with open neural folds and anomalous tailbuds with the brain system lacking sensitive spots are obtained.

(d) $Ph_2SnMetHis$ in 10^{-5} M solution exerts an intermediate effect since anomalous tailbuds and in 10^{-7} M solution anomalous larvae with twisted tails are observed (Figs 8c and 8d).

As a possible mechanism explaining the altered embryonic development observed mainly with the nBu_2Sn-derivative, we suggest that the concurrence of factors previously observed in a similar study on a Bu_2Sn-carbohydrate toxicant[39,40] operates also in our systems: there is probably a perturbation on the surface molecules of the plasma membrane and/or on the cytoskeleton, which blocks mitosis and inhibits cell movement and recognition at the gastrula stage, giving rise to anomalous embryos. Moreover, neurulae with open neural folds could be caused by the involvement of the microfilaments of neural-fold cells by the toxicants; this might bear some similarity to the neurotoxicity exerted by organotins in humans.[41]

CONCLUSION

The amphiphilic dipeptide H_2MetHis, in the complex $Me_2SnMetHis$, appears to adopt a self-assembly pattern, mediated by solvent molecules, by which the hydrophobic 'tail' (methionine) serves to align the monomeric units, while the hydrophilic 'head group' (histidine) forms a distinct structural motif (coordination to the organometallic moiety) where the 5-imidazolyl group is projected as a pendant arm on the exterior part of the complex providing self-association by an extensive network of H bonds, and offering a potential site for cell recognition. Spectroscopic studies agree with the suggestion that a similar structure is present in the nBu_2Sn^{2+} and Ph_2Sn^{2+} derivatives. Biological activity is closely related to that of previously investigated R_2Sn dipeptide complexes, in that the nBu_2Sn(IV) derivative appears to be more toxic. Among potential applications of the title compounds, it is worth noting that the dipeptide being the structural component which may recognize biologically relevant systems, DNA fixation of the organometallic moiety may be synergically induced.

Acknowledgements Financial support by the Ministero per l'Università e la Ricerca Scientifica e Tecnologica, Rome, is gratefully acknowledged.

REFERENCES

1. Tian ZQ, Bartlett PA. *J. Am. Chem. Soc.* 1996; **118**: 943.
2. (a) Fitzsimons MP, Barton JK. *J. Am. Chem. Soc.* 1997; **119**: 3379; (b) Sardesai NY, Zimmermann K, Barton JK. *J. Am. Chem. Soc.* 1994; **116**: 7502.
3. (a) Gielen M, Lelieveld P, de Vos D, Williem R. In Vitro Antitumor Activity of Diorganotin Compounds. In *Metal-Based Antitumor Drugs*, Vol. 2, Gielen M, (ed). Freund: London, 1992; 29–54, and references therein; (b) Saxena AK, Huber F. *Coord. Chem. Rev.* 1989; **95**: 109.
4. (a) Sóvágó I, Petöcz G. *J. Chem. Soc. Dalton Trans.* 1987; 1717; (b) Fröhling CDW, Sheldrick WS, *J. Chem. Soc. Dalton Trans.* 1997; 4411.
5. Smith MC, Furman TC, Pidgeon C. *Inorg. Chem.* 1987; **26**: 1965.
6. Schoeneich C, Zhao F, Wilson GS, Borchardt RT. *Biochim. Biophys. Acta* 1993; **1158**: 307.
7. Perlstein J, Steppe K, Vaday S, Ndip EM. *J. Am. Chem. Soc.* 1996; **118**: 8433, and references therein.
8. Girasolo MA, Pellerito L, Stocco GC, Valle G. *J. Chem. Soc. Dalton Trans.* 1996; 1195.
9. Elrod-Erickson M, Benson TE, Pabo CO. *Structure* 1998; **6**: 451, and references therein.
10. Berrill NJ. *The Tunicata*. Ray Society: London, 1950.
11. (a) Sheldrick GM. SHELX 86, Program for Solution of Crystal Structures. University of Göttingen, 1986; (b) Sheldrick GM. SHELX 76, Program for Crystal Structure Determination. University of Cambridge, 1976.
12. Johnson CK. ORTEP, Report ORNL-3794. Oak Ridge National Laboratory: Oak Ridge, TN, 1965.
13. (a) Madden JJ, McGandy EL, Seeman NC, Harding MM, Hoy A. *Acta Crystallogr. Sect. B* 1972; **28**: 2382; (b) Fuess H, Hohlwein D, Mason SA. *Acta Crystallogr. Sect. B* 1997; **33**: 654.
14. IUPAC–IUB Commission on Biochemical Nomenclature. *Biochemistry* 1970; **9**: 3471.
15. Stocco GC, Gulì G, Valle G. *Acta Crystallogr. Sect. C* 1992; **48**: 2116.
16. Jeffrey GA, Lewis L. *Carbohydr. Res.* 1978; **60**: 179.
17. Taylor R, Kennard O. *Acta Crystallogr. Sect. B* 1983; **39**: 133.
18. Miyasaka H, Okamura S, Nakashima T, Matsumoto N. *Inorg. Chem.* 1997; **36**: 4329.
19. Wong AK, Jacobsen MP, Winzor DJ, Fairlie DP. *J. Am. Chem. Soc.* 1998; **120**: 3836, and references therein.
20. Schenck HL, Dado GP, Gellman SH. *J. Am. Chem. Soc.* 1996; **118**: 12487.
21. Sundaralingham M, Sukharudu YC. *Science* 1989; **244**: 1333.
22. Perczel A, McAllister MA, Csaszar P, Csizmadia IG. *J. Am. Chem. Soc.* 1993; **115**: 4849.
23. Perczel A, Farkas O, Csizmadia IG. *J. Am. Chem. Soc.* 1995; **117**: 1653.
24. Gulì G, Gennaro G, Pellerito L, Stocco GC. *Appl. Organomet. Chem.* 1993; **7**: 407.
25. Mundus-Glowachki B, Huber F, Preut H, Ruisi G, Barbieri R. *Appl. Organomet. Chem.* 1992; **6**: 83.
26. Preut H, Mundus-Glowachki B, Huber F, Barbieri R. *Acta Crystallogr. Sect. C* 1989; **45**: 728.
27. Deacon GB, Phillips RJ. *Coord. Chem. Rev.* 1980; **33**: 227.
28. Reynolds WF, Peat IR, Freedman MH, Lyerla JR. *J. Am. Chem. Soc.* 1973; **95**: 328.
29. Shimba N, Takahashi H, Sakakura M, Fujii I, Shimada I. *J. Am. Chem. Soc.* 1998; **120**: 10988.
30. Lockart TP, Manders WF. *J. Am. Chem. Soc.* 1987; **109**: 7015.
31. Holecek J, Lycka A. *Inorg. Chim. Acta* 1986; **118**: L15.
32. Wüthrich K. *NMR of Proteins and Nucleic Acids*. Wiley–Interscience: New York, 1986.
33. Surdy P, Rubini P, Buzás N, Henry B, Pellerito L, Gajda T. *Inorg. Chem.* 1999; **38**: 346.
34. Rabenstein DL, Daignault SA, Isab AA, Arnold AP, Shoukry MM. *J. Am. Chem. Soc.* 1985; **107**: 6435.
35. Hawkins CJ, Martin J. *Inorg. Chem.* 1986; **25**: 2146.
36. Vestues PI, Martin RB. *J. Am. Chem. Soc.* 1980; **102**: 7906.
37. Lockhart TP, Manders WF. *Inorg. Chem.* 1986; **25**: 892.
38. Mansueto C, Lo Valvo M, Pellerito L, Girasolo MA. *Appl. Organomet. Chem.* 1993; **7**: 95.
39. Mansueto C, Pellerito L, Girasolo MA. *Acta Embryol. Morphol. Exper.* 1989; **10**: 237.
40. Mansueto C, Gianguzza M, Dolcemascolo G, Pellerito L. *Appl. Organomet. Chem.* 1993; **7**: 391.
41. Arakawa Y, Wada O. Biological Properties of Alkyltin Compounds. In *Metal Ions in Biological Systems*, Vol.29, Sigel H, Sigel A (eds). Marcel Dekker: New York, 1993; 101–136.

